Analyzing Impact of Network Constraints on Feasible Operation Region of the Radial Distribution Networks

Akhtar Hussain Javed⊙ ,Bart van der Holst, Phuong H. Nguyen, Johan Morren, J.G. Slootweg
Department of Electrical Engineering, Eindhoven University of Technology, Eindhoven, The Netherlands
a.h.javed, b.v.d.holst, p.nguyen.hong, j.morren, j.g.slootweg
@tue.nl

Abstract—Recently, there has been lot of research on finding the feasible operating region (FOR) of the active distribution network (ADN) to provide ancillary services to the transmission grid. The current focus of research is on finding methods that can accurately determine the shape of the FOR and have fast computation time. However, there is little focus on analyzing how network constraints impact the shape of the FOR. This paper attempts to address this issue and provides a mathematical derivation of how network constraints, such as cable loading and voltage limits, would influence FOR. The approach is based on a linear distflow mathematical analysis. The relations derived in the analysis are verified with numerical simulation on radial low-voltage (LV) and medium-voltage (MV) networks. The results show that cable loading constraints cut the FOR in a circular way and voltage constraints cut the FOR with a straight line of slope $-\epsilon$, which is the ratio R_n/X_n of the path from root node to the node under analysis of the radial distribution network.

Index Terms—TSO-DSO coordination, distribution system flexibility, ancillary services, power system planning, active distribution network

I. INTRODUCTION

Power systems have undergone numerous changes in recent years as a result of the ongoing energy transition. One of these changes is the replacement of synchronous generators in the transmission system by distributed energy resources (DERs) in the distribution system. Due to these changes, there is now a lack of controllable reactive power and inertia in the transmission grid [1], [2]. Similarly, additional developments in distribution grids like the conversion of overhead lines to underground cables, the changing nature of loads, installation of heat pumps, and the use of electric vehicles (EVs) have created several operational challenges for the system operators, including congestion[3], voltage fluctuations[4] and flows of capacive reactive power [5].

Distribution network with high penetration of power electronics interfaced renewable energy can provide flexibility [6]. Active and reactive power flexibility available from the DERs and flexible loads connected in the active distribution networks (ADNs) can be used to solve local issues in the distribution grid, and aggregated flexibility of the distribution system can be used to provide ancillary services to the transmission system. The ability of the ADN to provide active and reactive power flexibility to the transmission grid can be presented via the P-Q capability charts at the TSO/DSO (T-D) interface [7]. This aggregated capacity is normally communicated through the feasible operating region (FOR). Recently, there have been lot of research to find FOR for ADNs [8], [9], [10], [11], [12]. A review of methods for finding the FOR at the T-D interface is given in [13].

The methods available in literature for computing FOR can be categorized as *(i)* power flow based methods *(ii)* optimal power flow (OPF) or optimization based methods *(iii)* geometrical approaches and *(iv)* analytical methods. Having fast estimation of flexibility is very important for real time operation and control of power system [14]. The importance of fast flexibility assessment is also highlighted in universal smart energy framework (USEF) [15]. The article [16] presents a comparison of the computational times for various OPF formulations used to determine the FORs. This comparison demonstrates that the LinDistflow method leads to quicker computation of FOR. In [17], a comparison is conducted between a random sampling-based approach and proposed interval constrained power flow (ICPF) in terms of FOR computation time. The study demonstrates that as the number of samples increase, ICPF outperforms the random sampling method on parameters of reduced computation time and % flexibility area increase. There are very few analytical approaches for flexibility assessment at T-D interface [11] [18] but they are normally very fast because analytical approaches are based on equations and take less time to compute.

The FOR of a network is influenced by many factors, for example: topology of the network, tap change of transformer, DER capabilities, and network constraints among others. Most of the methods available in the literature usually focus on finding FOR without explicitly analyzing the impact of the above factors on the shape of FOR. In [19] and [20] attempts are made to find out how network topology and tap position of on load tap changer (OLTC) affects FOR. However, there is very little literature that fundamentally analyzes how network
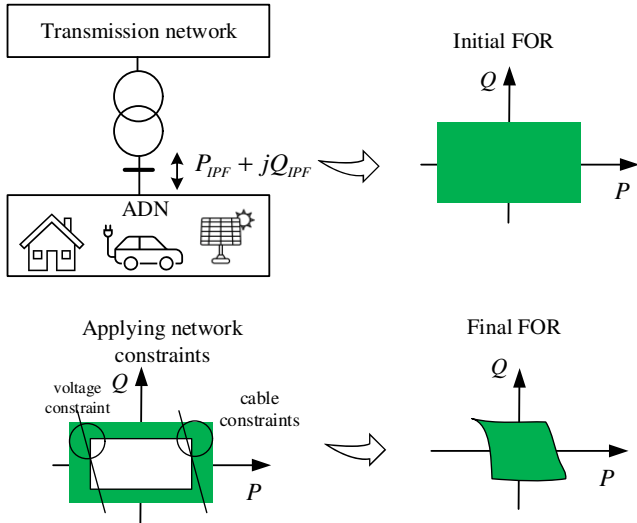
Fig. 1. Overview of the method used for analyzing network constraint's impact on FOR

Require: Network constraint, flexible loads and generation
    Create $n \in N$ load and generation (p,q) operation points uniformly by changing their p, q values from 0 to 1 pu
    for $n \leftarrow 1$ to N **do**
        Run power flow and find IPF
        if any network constraints are violated **then**
            Discard IPF
        else
            Add corresponding IPF to the FOR
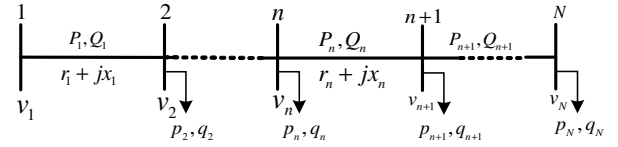   **end if**
    end for
Output: FOR

Fig. 2. Single line diagram of a simplified distribution feeder

constraints influence the shape of FOR. In this work an attempt is made in this regard to analyze how cable loading and voltage constraints of the network influence the shape of the FOR.

The main contributions are as follows.

- Finding a simplified mathematical formulation which can depict influence of both cable loading and voltage constraints on the shape of the FOR
- Validating the mathematical analysis through numerical simulation on LV and MV radial distribution network

The rest of the paper is structured as follows: An outline of the research methodology is provided in Section II. Complete mathematical formulation along with analytical analysis is presented in section III. The numerical simulation in Section IV is used to validate the results of the mathematical analysis. Section V consists of a conclusion and a recommendation for future work.

II. METHODOLOGY

An overview of the methodology used in the paper is given here. First, the initial FOR of the given ADN is computed. This initial FOR is the combination of all possible active and reactive power flows at the beginning of the feeder, also called interconnection power flows (IPFs) [7] without applying any network constraints. This initial FOR consists of both feasible and infeasible IPFs. Feasible here means that no network constraint is violated resulting in that IPF. Infeasible means that there are active and reactive values of loads and DERs which result in the IPF such that a network constraint is violated. To remove IPFs that are infeasible, cable loading and nodal voltage constraints are applied on the initial FOR, which would cut some parts of the FOR. The remaining approximated area is the final FOR obtained through our analysis. This procedure is explained in Fig. 1. This final FOR obtained through analysis is then compared with the exact FOR, which is calculated by running power flows and removing all points that result in any network constraints violations. The algorithm 1, describes the method used for

finding exact FOR. The analysis which is the main contribution of this work is presented in the next section.

III. MATHEMATICAL ANALYSIS

In this section, we will derive the analytical expressions for the boundaries of the FORs due to cable capacity and voltage constraints in a radial distribution network. The linearized distflow approach [21] is selected because it results in faster computation and has a reasonable level of accuracy for distribution system. First, analytical equations are derived for the power flows in the branches and the voltages at the nodes. Then we impose cable capacity constraints and voltage constraints and interpret the resulting inequalities geometrically in terms of the FOR. The analysis is divided into two parts. First, an analysis is presented for a simple network without branches. Subsequently, the analysis is generalized to radial distribution networks.

A. Analytical solution to the linearized Distflow equations

Let's assume that in the beginning we have a three phase balanced simplified radial network as shown in Fig.2. The network consists of N nodes and $N-1$ branches. All nodes have active and reactive power loads or injections represented as (p_n, q_n) except for the node 1 which is the root node. The power flows of the nth branch in the network are represented as P_n and Q_n. The nodal voltages in the network are represented as v_n. The impedance of each branch is given as $r_n + jx_n$. If we use linearized Distflow , the powerflows in the branch $n + 1$ can be expressed as

$$P_{n+1} = P_n - p_{n+1} \tag{1}$$

$$Q_{n+1} = Q_n - q_{n+1} \tag{2}$$
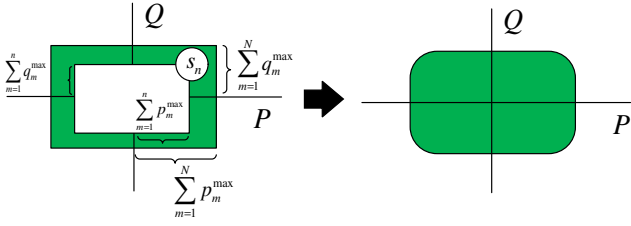
$$v_{n+1}^2 = v_n^2 - 2r_n P_n - 2x_n Q_n \tag{3}$$

Fig. 3. Cable constraint cut of the FOR (green) as a result of equation (7)

Fig. 4. The voltage constraints cuts the FOR with slope $-R_n/Xn$ as in equations (13),(14)

Here, we adopted the convention that for e.g. the consumption of active power at node n we have $p_n \geq 0, q_n \geq 0$, and that power flowing away from the root node is positive.

To derive an analytical expression of the grid constraints for FOR, we should express P_n, Q_n and v_n in terms of P and Q. Subsequently, we can visualize the equations in the $P-Q$ plane. We can first solve the above equation for active and reactive power flows. We can write power flows for any n^{th} branch as

$$P_n = P - \sum_{m=1}^{n} p_m \qquad (4)$$

$$Q_n = Q - \sum_{m=1}^{n} q_m \qquad (5)$$

Where P and Q here represent the $P-Q$ of the FOR plane which is sum of all flows at the beginning of the feeder.

1) Cable Constraints in the $P-Q$ plane: The cable constraints of the network can be written as

$$P_n^2 + Q_n^2 \leq s_n^2 \qquad (6)$$

where P_n, Q_n are the active power and reactive power flows in the branch and s_n is the cable rating for that particular branch. This equation can be written to express cable loading constraints on the $P-Q$ region using eq.(4) and eq.(5) as:

$$(P - \sum_{m=1}^{n} p_m)^2 + (Q - \sum_{m=1}^{n} q_m)^2 \leq s_n^2 \qquad (7)$$

This equation is similar to $(x-a)^2 + (y-b)^2 = r^2$ which is the equation for the circle in which center point is (a, b) and r is radius. Equation 7 represents cable loading as a circle in which the radius of the circle is the cable capacity s_n and the center of the circle is $(\sum_{m=1}^{n} p_m, \sum_{m=1}^{n} q_m)$. If we plot this on FOR we can see how cable loading constraints impact the FOR. Fig.3 shows that cable loading constraints would cut the FOR in a circular way. Note that there would be a set of circles given by equation(7), here for visualization only one circle is shown. To remove an infeasible point due to violation of cable loading constraints, we will check its distance from the center of circle, if it is more than s_n it would be an infeasible point and will not be the part of the FOR. For illustration, we can draw a rectangle with length of $\sum_{m=1}^{n} p_m^{max}$ and width of $\sum_{m=1}^{n} q_m^{max}$ as shown in Fig.3 and measure the distances from the center of the circles to the point. All powerflows outside the circle would result in exceeding cable loading limits and hence would not be the part of the FOR.
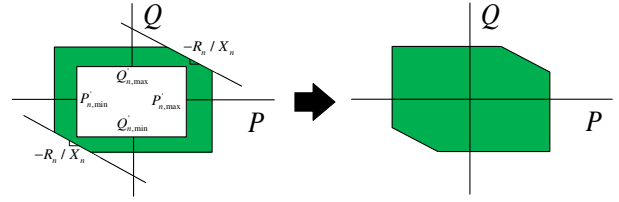
2) Voltage constraints in the $P-Q$ plane: For voltage constraints we assume that same voltage limits v_{min} and v_{max} holds for all nodes in the network. We then have the following set of voltage constraints:

$$v_{min}^2 \leq v_n^2 \leq v_{max}^2 \qquad (8)$$

For voltages, we express voltages in downstream nodes with respect to voltage at root node which is node 1, assuming $v_1 = v$ is the transformer lower side voltage. The voltage at any n^{th} node can then be expressed based on Eq.(3) knowing v_1

$$v_n^2 = v^2 - 2\sum_{m=1}^{n-1} r_m P_m - 2\sum_{m=1}^{n-1} x_m Q_m \qquad (9)$$

The sum terms in eq.(9) contains sum of linear voltage losses until nth node. It can be interpreted as the voltage at the nth node being the voltage at the beginning of the transformer minus the linear voltage losses. We again can write P_m, Q_m in eq.(9) in terms of P and Q based on eq.(4) and eq.(5) as follows:

$$v_n^2 = v^2 - 2\sum_{m=1}^{n-1} r_m(P - \sum_{k=1}^{m} p_k) - 2\sum_{m=1}^{n-1} x_m(Q - \sum_{k=1}^{m} q_k) \quad (10)$$

After substituting $R_n = \sum_{m=1}^{n-1} r_m$, $X_n = \sum_{m=1}^{n-1} x_m$ which is sum of all resistances and reactances until the nth node in above equation we get

$$v_n^2 = v^2 - 2R_n P - 2X_n Q + 2\sum_{m=1}^{n-1} r_m \sum_{k=1}^{m} p_k + 2\sum_{m=1}^{n-1} x_m \sum_{k=1}^{m} q_k \qquad (11)$$

Let's assume $\epsilon = \frac{R_n}{X_n}$ is the R/X ratio of the feeder from root node to the nth node. Dividing eq(11) by $2X_n$ and rearranging, we can represent voltage in the form P and Q as

$$\frac{v^2 - v_{max}^2}{2X_n} \leq (\epsilon P - P_n') + (Q - Q_n') \leq \frac{v^2 - v_{min}^2}{2X_n} \quad (12)$$

where $P_n' = \frac{1}{X_n}\sum_{m=1}^{n-1} r_m \sum_{k=1}^{m} p_k$ and $Q_n' = \frac{1}{X_n}\sum_{m=1}^{n-1} x_m \sum_{k=1}^{m} q_k$. Eq.(12) describes linear cuts in the P-Q plane. Rewriting the equations in terms of Q to get linear cut equations, we get:

$$Q \leq Q_n' + \frac{v^2 - v_{min}^2}{2X_n} + P_n' - \frac{R_n}{X_n}P \qquad (13)$$

$$Q \geq Q_n' + \frac{v^2 - v_{max}^2}{2X_n} + P_n' - \frac{R_n}{X_n}P \qquad (14)$$
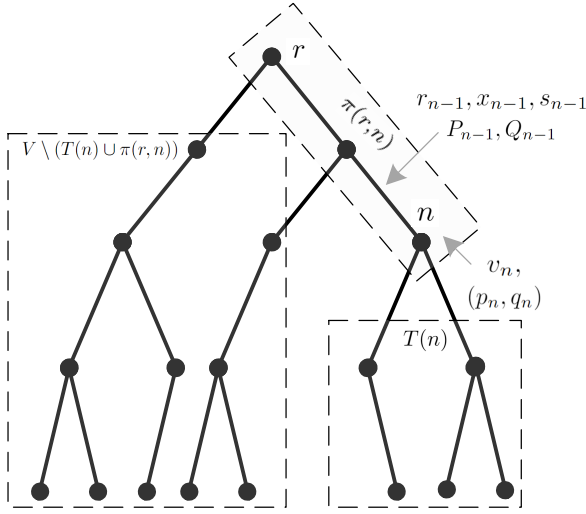
Fig. 5. The oriented tree graph with the notations used throughout the paper.

Fig.4 shows how voltage constraints would cut the FOR. The voltage cuts have intercepts given by $Q'_n + \frac{v^2 - v^2_{min}}{2X_n} + P'_n$ and $Q'_n + \frac{v^2 - v^2_{max}}{2X_n} + P'_n$, while the slope is $-\frac{R_n}{X_n}P$.

B. Generalized analysis for radial distribution networks with branches

In the previous section, we found analytical expressions for network constraint's impact on FOR in simple networks without branches. In this section, we generalize the analysis for radial distribution grids. We consider a balanced three-phase radial feeder represented by an oriented simple tree graph $G = (V, E)$ with vertices V and edges E. Let $r \in V$ be the root node, which is at the beginning of the feeder. With every node we associate a voltage magnitude v_n and a dispatchable load (p_n, q_n) in some compact (bounded and closed) operating region $S_n \subset \mathbb{R}^2$. With each edge, representing a cable, we associate an impedance $r_n + jx_n$, capacity s_n, active power flow P_n, and reactive power flow Q_n, where n denotes the edge node closer to the root node r as shown in Fig. 5. We also denote the flows through the root node simply by P and Q and its voltage by v. Note that we adopt the same notation conventions as in Section III-A. For the relation between v_n, p_n, q_n, P_n and Q_n we consider again the linearized distflow equations for all $n \in V$, similar to equations (1)-(3), but now for general radial networks:

$$\sum_{k:n+1 \to k} P_k = P_n - p_{n+1}$$
$$\sum_{k:n+1 \to k} Q_k = Q_n - q_{n+1} \tag{15}$$
$$v^2_{n+1} = v^2_{k:k \to n+1} - 2r_n P_n - 2x_n Q_n$$

where e.g. $k : k \to n+1$ denotes the (unique) node which is the start of a cable to node $n + 1$.

If we take some node n and iterate the first two equations of (15) we realize that P_n and Q_n are the sum of the loads in the subtree of node n, where the subtree $T(n) \subset V$ of node n refers to the set of nodes behind n with respect to r (see

Fig. 5). From this result again follows that P and Q are the total sums of the loads, and we can express P_n and Q_n in terms of P and Q by subtracting the sum over all loads in the complement of $T(n)$:

$$P_n = P - \sum_{m \in V \setminus T(n)} p_m \qquad \forall n \in V$$
$$Q_n = Q - \sum_{m \in V \setminus T(n)} q_m \qquad \forall n \in V, \tag{16}$$

which is the more general form of equations (4)-(5). For the voltages, we iterate the voltage law in equation (15) from the root node along the path from the root node to n. Note that in tree graphs there is only one unique path between two nodes. Let the nodes within the path between two nodes n and m be denoted by $\pi(n, m)$. We then obtain a similar equation to (9):

$$v^2_n = v^2 - 2\sum_{m \in \pi(r,n)} r_m P_m - 2\sum_{m \in \pi(r,n)} x_m Q_m \qquad \forall n \in V. \tag{17}$$

We can now plug equations (16) in equation (17), but it is insightful to split the nodes in the set $V \setminus T(n)$ in nodes being part of $\pi(r, n)$ and the ones that are not. Note that the nodes part of $\pi(r, n)$ are always part of $V \setminus T(n)$, because they are never in the subtree of node n. The remaining nodes $V \setminus (T(n) \cup \pi(r, n))$ are all nodes in other branches than n is part of (see Fig. 5). Let us also define the quantity $R_n = \sum_{m \in \pi(r,n)} r_m$, as the total resistance between the root node and node n. If we then focus on the second term on the right-hand side of equation (17) we obtain:

$$2\sum_{m \in \pi(r,n)} r_m P_m = 2R_n P - 2\sum_{m \in \pi(r,n)} r_m \left(\sum_{l \in \pi(r,m)} p_l \right)$$
$$- 2\sum_{m \in \pi(r,n)} r_m \left(\sum_{l \in V \setminus (T(m) \cup \pi(r,m))} p_l \right) \tag{18}$$

This equation simply shows that the voltage drop due to active power flow between nodes r and n can be calculated by assuming that all power flow in the network goes through the cable along the path, corrected for the voltage drop due to the loads in the path, and with the power flowing to other branches in the network. The last part is not present in the analysis of section III-A. A very similar relation can be obtained for the voltage drop due to reactive power. We now will apply these relations to study the line and voltage constraints in the $P-Q$ plane for a branched network.

1) Cable Constraints in the $P - Q$ plane: The cable constraints for the network can again be written as:

$$P^2_n + Q^2_n \leq s^2_n, \qquad \forall n \in V \tag{19}$$

which can be written as a similar set of constraints on P and Q as (7) using equation (16) as follows:

$$\left(P - \sum_{m \in V \setminus T(n)} p_m \right)^2 + \left(Q - \sum_{m \in V \setminus T(n)} p_m \right)^2 \leq s^2_n \qquad \forall n \in V \tag{20}$$

for all possible loading conditions of loads $m \in V \setminus T(n)$. Geometrically, these equations represent a set of circles in the $P - Q$ plane of radius s_n with its centers at the sum of the loads not in the subtree of node n. Given some FOR, this set of equations cuts away points in the region if there is no $n \in V$ and no circle center for which the point satisfies equation (20). Notice that the main intuitions behind the cable constraints do not change compared to the linear network case discussed in III-A1. We note that if the cable capacity s_n is large enough, all points within the original FOR satisfy the cable loading constraint, and that no points get cut away. Also note that if we consider nodes closer to the feeder that the region $S_{N \setminus T(n)}$ becomes smaller as more nodes lie in its subtree, but the cable capacities typically become larger.

2) Voltage Constraints in the $P - Q$ plane: For the voltage constraints, we again assume equation (8) holds. To express these constraints in terms of P and Q, we use equations (17), (18) and its similar version for reactive power to obtain:

$$\frac{v^2 - v_{max}^2}{2X_n} \leq (\epsilon P - P_n') + (Q - Q_n') \leq \frac{v^2 - v_{min}^2}{2X_n}, \quad (21)$$

which is the same as equation (12). However, P_n' and Q_n' are now expanded with an extra term due to the network being branched:

$$
P_n' = \frac{1}{X_n} \sum_{m \in \pi(r,n)} r_m \left(\sum_{l \in \pi(r,m)} p_l \right) \\
+ \frac{1}{X_n} \sum_{m \in \pi(r,n)} r_m \left(\sum_{l \in V \setminus (T(m) \cup \pi(r,m))} p_l \right), \quad (22)
$$

and:

$$
Q_n' = \frac{1}{X_n} \sum_{m \in \pi(r,n)} x_m \left(\sum_{l \in \pi(r,m)} q_l \right) \\
+ \frac{1}{X_n} \sum_{m \in \pi(r,n)} x_m \left(\sum_{l \in V \setminus (T(m) \cup \pi(r,m))} q_l \right) \quad (23)
$$

The equation (21) thus represents the same linear cuts given as (13) and (14) as derived earlier in section III-A2. Notice that again the slope of the linear cuts is given by $-R_n/X_n$. The intercept of the cuts is different now as for the linear network case as P_n' and Q_n' contain an additional term. Again, the voltage cuts should remove the points of the FOR if there is a condition that violates the grid constraints. This implies that we should apply the loosest voltage cuts to the FOR that still satisfy equations (13) and (14). We observe that this requires us to the maximum/minimum intercept for the linear cuts for the minimum/maximum voltage constraints in the nodes respectively, and hence the maximum/minimum values for P_n' and Q_n' for the linear cuts for the minimum/maximum voltage constraints in the node respectively. Let us now assume that all S_n are rectangular operating regions such that all linear combinations of operating regions are rectangular regions as well. For the minimum voltage constraints (13) this means

that both P_n' and Q_n' should be at their maximum value (maximum consumption) to provide the weakest bound on the FOR. For the maximum voltage constraints (14), this means that both P_n' and Q_n' should have a minimum value (maximum generation). Let $p_{n,min}, p_{n,max}$ and $q_{n,min}, q_{n,max}$ denote the minimum and maximum values of active and reactive power in a rectangular operating region S_n at node $n \in V$. In that case, we have the following.

$$Q \leq Q_{n,max}' + \frac{v^2 - v_{min}^2}{2X_n} + P_{n,max}' - \frac{R_n}{X_n} P \quad (24)$$

$$Q \geq Q_{n,min}' + \frac{v^2 - v_{max}^2}{2X_n} + P_{n,min}' - \frac{R_n}{X_n} P \quad (25)$$

where:

$$
\begin{aligned}
P_{n,min}' &= \frac{1}{X_n} \sum_{m \in \pi(r,n)} r_m \left(\sum_{l \in \pi(r,m)} p_{l,min} \right) \\
&\quad + \frac{1}{X_n} \sum_{m \in \pi(r,n)} r_m \left(\sum_{l \in V \setminus (T(m) \cup \pi(r,m))} p_{l,min} \right) \\
P_{max,n}' &= \frac{1}{X_n} \sum_{m \in \pi(r,n)} r_m \left(\sum_{l \in \pi(r,m)} p_{l,max} \right) \\
&\quad + \frac{1}{X_n} \sum_{m \in \pi(r,n)} r_m \left(\sum_{l \in V \setminus (T(m) \cup \pi(r,m))} p_{l,max} \right) \\
Q_{n,min}' &= \frac{1}{X_n} \sum_{m \in \pi(r,n)} x_m \left(\sum_{l \in \pi(r,m)} q_{n,min} \right) \\
&\quad + \frac{1}{X_n} \sum_{m \in \pi(r,n)} x_m \left(\sum_{l \in V \setminus (T(m) \cup \pi(r,m))} q_{n,min} \right) \\
Q_{n,max}' &= \frac{1}{X_n} \sum_{m \in \pi(r,n)} x_m \left(\sum_{l \in \pi(r,m)} q_{n,max} \right) \\
&\quad + \frac{1}{X_n} \sum_{m \in \pi(r,n)} x_m \left(\sum_{l \in V \setminus (T(m) \cup \pi(r,m))} q_{n,max} \right)
\end{aligned} \quad (26)
$$

C. Result of Mathematical Analysis

In this subsection we summarize the results of our mathematical analysis. The summary of the analysis is as following:

- Cable loading constraints can be represented by a set of circles. The radius of these circles is the cable loading capacity s_n. If the powerflow in the cable is within the limit there would be not cut on the FOR. If the cable is loaded beyoned its capacity the cable loading constraint would cut the FOR in a circular way.
- The FOR is limited by voltage constraints in the shape of a straight line. The gradient of this line is $-\epsilon$, which is the R/X ratio of the path from the root node to the node under analysis.
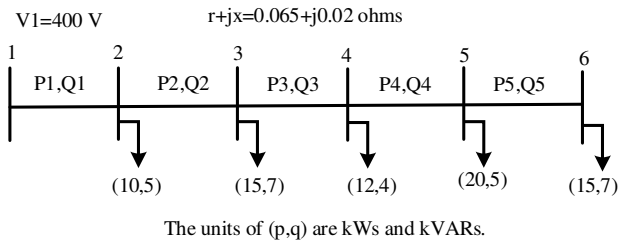
V1=400 V   r+jx=0.065+j0.02 ohms

The units of (p,q) are kWs and kVARs.

Fig. 6. LV network used for numerical simulation and FOR analysis

IV. NUMERICAL VERIFICATION OF THE MATHEMATICAL ANALYSIS BY POWER FLOW BASED FOR

In this section, numerical simulations are performed to verify the results of mathematical analysis.

A. Low voltage network with flexible loads

For a clearer demonstration of how network constraints affect FOR, we first apply the aforementioned mathematical analysis to a straightforward low voltage radial distribution network, shown in Fig.6, which consists of flexible loads. The network consists of six nodes and five branches. Here, we assume that the impedance of all branches is the same given as $0.065 + j0.02$ ohms. The voltage of the first node is set as $v_1 = 400V$. The loads at each node are given as (p_n, q_n) with active and reactive power values in kW and kVar. As illustrated in Fig.1, for analysis, the first step is to find the network's initial FOR, which is calculated by increasing the active and reactive power values of flexible loads from 0 to 1 pu and calculating IPF. Since our network consists only of flexible loads, we get the initial FOR in first quadrant. The resulting initial FOR which is the result of all possible IPFs is shown in Fig.7. Note that this initial FOR consists of both feasible and infeasible points. We will apply our linear analysis on top of this FOR to remove points that are infeasible. Next step is to apply cable loading and voltage constraints. The voltage constraint analysis would be quite straightforward because our network is radial and solely consists of loads, only the constraint v_{min} given in equation (13) would apply. Furthermore, due to the properties of the radial network, we only need to plot the voltage cut of the final node. However, cable loading constraints of each branch need to be separately examined for the purpose of analysis.

1) Analysis on branch 5: For analysis on branch 5, first we plot the inner region which is rectangular shape given by equations (4),(5) $P_5 = P - \sum_{m=1}^{5} p_m, Q_5 = P - \sum_{m=1}^{5} q_m$. The cable loading constraint is then plotted in the form of circle. The center of circle for branch five is given by $(\sum_{m=1}^{5} p_m, \sum_{m=1}^{5} q_m)$. The resulting analysis results are given in Fig.8. Actually, there would be infinite circles here for visualization, only one circle is plotted. The circle radius would be the loading capacity of the cable. The cable loading capacities for the network in this example are given in TableI. All the points inside the circle are following the cable loading constraints and would be part of the final FOR if they are not cut by voltage constraint. The points outside the circle do
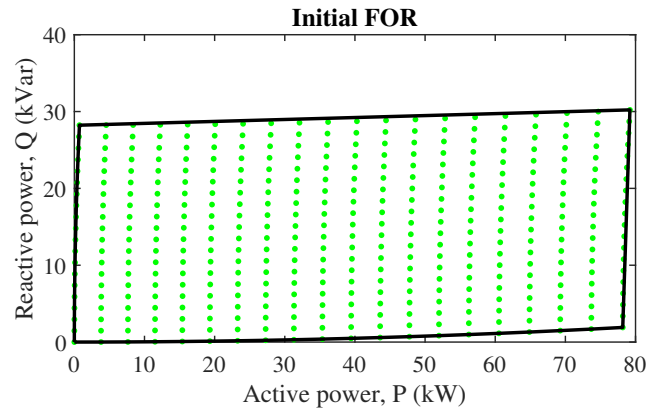

Fig. 7. Initial FOR wihtout network constraints applied

TABLE I
PARAMETERS FOR ANALYSIS OF LV NETWORK

Branch no	Cable capacity (kVA)	Circle center	P'_n	Q'_n
1	150	(0,0)	0	0
2	150	(10,5)	6.5	1
3	100	(25,12)	22.75	3.4
4	50	(37,16)	46.8	6.6
5	22	(57,21)	83.85	10.8

not follow cable loading constraints and hence would not be included in the final FOR. After this, voltage constraints of the network are applied using equation (13) in which reactive power is expressed as a straight line in form of active power with slope of $-R_n/X_n$. In equation (13), P'_n, Q'_n, $v = 400V$ and $v_{min} = 360V$ are constant values. After calculating P'_n, Q'_n and other values given in tableI, the voltage cut is plotted on the initial FOR. The voltage constraints cut the FOR with a slope $-R_n/X_n = -3.25$ as shown in the red line in Fig.8. The FOR after this stage would be the one cut by voltage constraints since the area cut by cable loading constraints is already included in the area cut by voltage constraints.

2) Analysis on other branches and final FOR obtained through analysis: We don't need to apply voltage constraints for other nodes due to network's radial property. However, for cable loading constraints, a similar analysis will be applied for all other branches of the network. The resulting parameters and center of circles for loading constraints are given in tableI. The
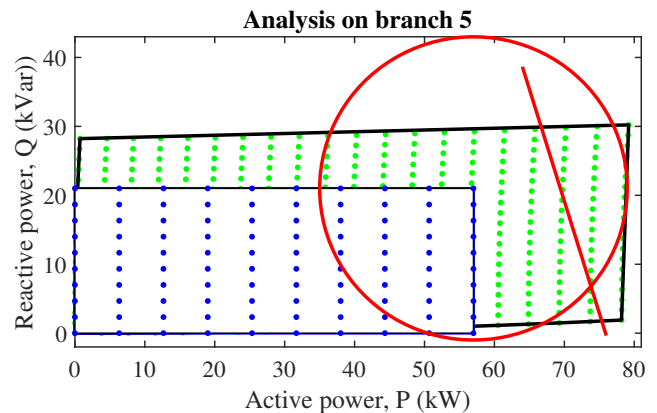

Fig. 8. Applying loading constraints on branch 5 and voltage constraints on node 6
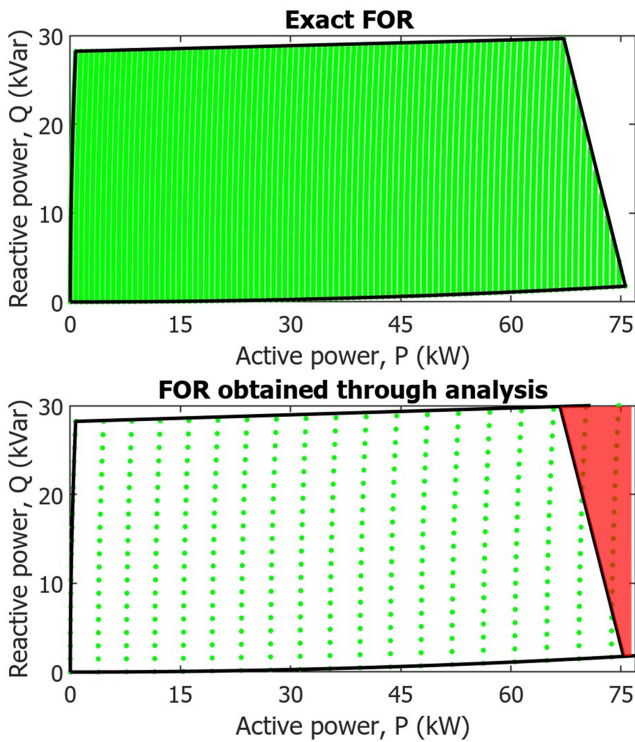
Fig. 9. Comparison of exact FOR obtained by algorithm 1 (top) and FOR obtained with mathematical analysis for the LV network (bottom)

Fig. 11. Comparison of exact FOR for modified case 22 radial network obtained by algorithm 1 (top) and FOR obtained by analysis (bottom)
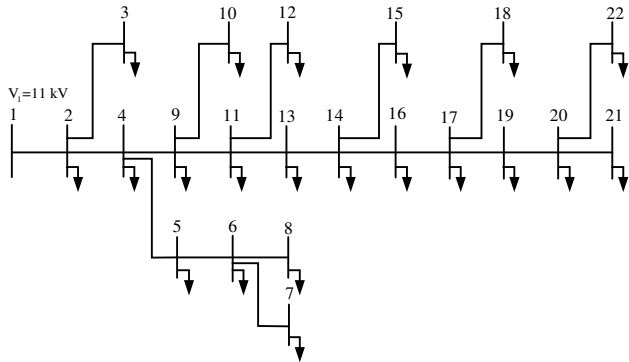

Fig. 10. MV network used for numerical simulation of FOR analysis

resulting FOR after applying all network constraints and the exact FOR obtained by the power flow method are given in Fig.9. It can be seen that final FOR obtained by our analysis is quite similar to the exact FOR obtained by powerflow method. This shows the efficacy of our method.

B. Medium voltage network with flexible loads

In this subsection, mathematical analysis is applied to a IEEE modified case 22 radial distribution network in MAT-POWER [22]. The MV network used is shown in Fig. 10. The base voltage level of this network is 11 kV. The impedance of all the branches is set as $2.75 + j1$ ohms. There is no load connected on bus 1 which is the root node. Values of active and reactive power flexible loads connected to the network are given in the table.II. To simplify the analysis, the cable capacity is set high enough to avoid any violation of the cable loading constraint. The primary emphasis of the analysis is on voltage constraints. A method similar to the
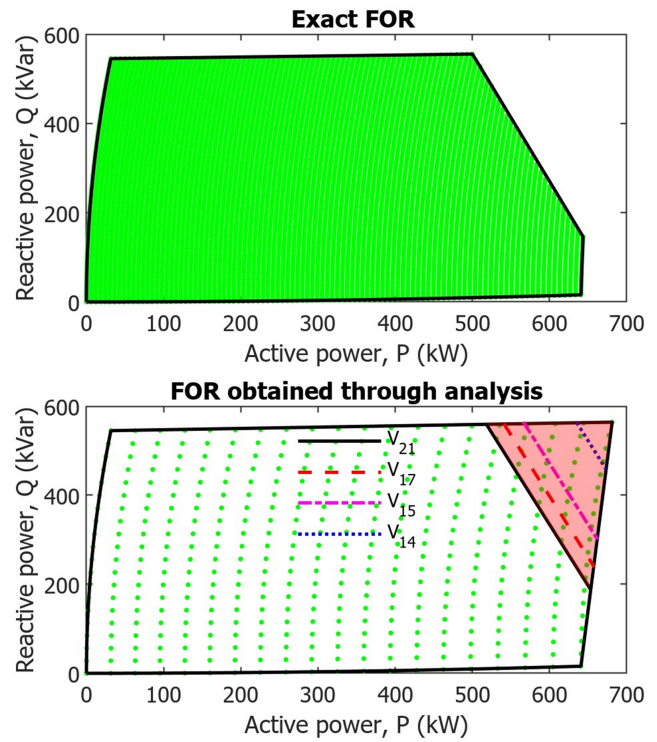
method in the previous subsection for LV network analysis is employed for the analysis. First, the initial FOR of the MV network is calculated. Then voltage constraints are applied. Since this network consists only of flexible loads, there would be a violation of the minimum voltage. For the purpose of the analysis, v_{min} is set as $0.9V_{base}$. Equation (24) derived from constraints v_{min} for radial networks is used here to find the cut in the initial FOR. This equation removes the part of the initial FOR that would result in a any violation of the voltage constraints. The final FOR obtained through analysis along with the exact FOR is outlined in Fig.11. In FOR obtained through analysis portion of the Fig.11 voltage cuts for nodes 14, 15, 17 and 21 are also plotted. Similar cuts could be drawn for all nodes in the network. Nodes that have a voltage lower than v_{min} would cut the FOR. To identify FOR, it is not essential to plot the voltage cut for each node; instead, only the node with the lowest voltage, in this case node 21, needs to be shown. The final FOR obtained through analysis is close to exact FOR. However, if we look at Fig.11 in detail, we can observe that there is some mismatch in exact FOR and FOR obtained through analysis. This is because our analysis is based on the linearized distflow method, which ignores quadratic losses. In future work, the accuracy of the method can be increased by adding quadratic losses to the formulation. Moreover, the exact FOR which is used in this paper to compare accuracy of our method can also be further improved. The accuracy of exact FOR is influenced by the sampling technique and the amount of samples used to determine it. With increasing the number of samples, the exact FOR obtained would be much closer to our approximation of

Bus no	P_L(kW)	Q_L(kVAR)	Bus no	P_L(kW)	Q_L(kVAR)
1	0	0	12	10	5
2	16.78	20.91	13	82.13	71.65
3	10	5	14	34.71	30.12
4	33.80	37.32	15	34.71	30.12
5	10	5	16	80.31	70.12
6	10	5	17	49.62	47.82
7	10	5	18	10	5
8	10	5	19	43.77	38.93
9	19.31	25.87	20	37.32	35.96
10	10	5	21	37.32	35.96
11	16.27	19.48	22	31.02	29.36

the FOR. This aspect is worth exploring in future research.

1) Computation time comparison: The computational time calculations were conducted using MATLAB 2023b running on Windows 11 Enterprise with an Intel Core i7-9750H processor, operating at 2.60 GHz, and equipped with 16 GB of RAM. For exact FORs, 10,000 uniformly sampled combinations of (p, q) were used. Initial FOR used for finding FOR through analysis only used 400 combinations of (p, q) because the voltage limits and cable loading cuts were calculated by equations obtained through mathematical analysis. The computation time for LV network case study is only 19 seconds for FOR obtained through analysis compared to 435 seconds for exact FOR. For MV network case FOR obtained through analysis took only 47 seconds compared to 874 seconds for Exact FOR. The method proposed does better in computation time compared to exact FOR due to less number of samples needed.

V. CONCLUSION

This paper examines the influence of network constraints on FOR through analytical analysis. According to the results of analytical analysis, the cable loading constraints would cut the FOR in the form of circles with a radius equal to the cable kVA rating s_n and the nodal voltage constraints would cut the FOR with a straight line of slope $-R_n/X_n$. The mathematical analysis is then applied to two distribution networks to show the efficacy of the method. The results show that FOR obtained through mathematical analysis is a close approximation of the exact FOR obtained through powerflow based method. In applications where computation time is important, an approach based on this analysis can be used to compute the FOR. In order to increase the accuracy of the FOR found through analysis, further work would involve approximating quadratic losses which are neglected in our current approach and adding them to the mathematical formulation.

REFERENCES

[1] F. Capitanescu, "Evaluating reactive power reserves scarcity during the energy transition toward 100% renewable supply," *Electr. Power Syst. Res.*, vol. 190, no. March 2020, p. 106672, 2021. [Online]. Available: https://doi.org/10.1016/j.epsr.2020.106672

[2] F. Milano, F. Dörfler, G. Hug, D. J. Hill, and G. Verbič, "Foundations and challenges of low-inertia systems (invited paper)," in *2018 Power Systems Computation Conference (PSCC)*, 2018, pp. 1–25.

[3] S. Huang and Q. Wu, "Real-time congestion management in distribution networks by flexible demand swap," *IEEE Transactions on Smart Grid*, vol. 9, no. 5, pp. 4346–4355, 2018.

[4] A. H. Javed, P. H. Nguyen, J. Morren, and J. H. Slootweg, "Review of operational challenges and solutions for der integration with distribution networks," in *2021 56th International Universities Power Engineering Conference (UPEC)*, 2021, pp. 1–6.

[5] A. H. Javed, P. H. Nguyen, J. Morren, J. Han Slootweg, and S. Battacharyya, "Issues of capacitive reactive power flow in electricity networks," in *2022 57th International Universities Power Engineering Conference (UPEC)*, 2022, pp. 1–6.

[6] H. Früh, S. Müller, D. Contreras, K. Rudion, A. von Haken, and B. Surmann, "Coordinated vertical provision of flexibility from distribution systems," *IEEE Transactions on Power Systems*, vol. 38, no. 2, pp. 1834–1844, 2023.

[7] D. Mayorga Gonzalez, J. Hachenberger, J. Hinker, F. Rewald, U. Häger, C. Rehtanz, and J. Myrzik, "Determination of the time-dependent flexibility of active distribution networks to control their tso-dso interconnection power flow," in *2018 Power Systems Computation Conference (PSCC)*, 2018, pp. 1–8.

[8] M. Heleno, R. Soares, J. Sumaili, R. Bessa, L. Seca, and M. A. Matos, "Estimation of the flexibility range in the transmission-distribution boundary," in *2015 IEEE Eindhoven PowerTech*, 2015, pp. 1–6.

[9] J. Silva, J. Sumaili, R. J. Bessa, L. Seca, M. Matos, and V. Miranda, "The challenges of estimating the impact of distributed energy resources flexibility on the tso/dso boundary node operating points," *Computers and Operations Research*, vol. 96, pp. 294–304, 8 2018.

[10] S. Kundu, K. Kalsi, and S. Backhaus, "Approximating flexibility in distributed energy resources: A geometric approach," in *2018 Power Systems Computation Conference (PSCC)*, 2018, pp. 1–7.

[11] S. Stanković and L. Söder, "Analytical estimation of reactive power capability of a radial distribution system," *IEEE Transactions on Power Systems*, vol. 33, no. 6, pp. 6131–6141, 2018.

[12] S. Riaz and P. Mancarella, "On feasibility and flexibility operating regions of virtual power plants and tso/dso interfaces," in *2019 IEEE Milan PowerTech*, 2019, pp. 1–6.

[13] G. Papazoglou and P. Biskas, "Review of methodologies for the assessment of feasible operating regions at the tso–dso interface," *Energies*, vol. 15, no. 14, 2022. [Online]. Available: https://www.mdpi.com/1996-1073/15/14/5147

[14] J. Zhao, T. Zheng, and E. Litvinov, "A unified framework for defining and measuring flexibility in power system," *IEEE Transactions on Power Systems*, vol. 31, no. 1, pp. 339–347, 2016.

[15] "USEF: The framework explained," USEF Foundation, Arnhem, Netherlands. [Online]. Available: https://www.usef.energy/app/uploads/2021/05/USEF-The-Framework-Explained-update-2021.pdf

[16] L. Lopez, A. Gonzalez-Castellanos, D. Pozo, M. Roozbehani, and M. Dahleh, "Quickflex: a fast algorithm for flexible region construction for the tso-dso coordination," in *2021 International Conference on Smart Energy Systems and Technologies (SEST)*, 2021, pp. 1–6.

[17] J. Silva, J. Sumaili, R. J. Bessa, L. Seca, M. A. Matos, V. Miranda, M. Caujolle, B. Goncer, and M. Sebastian-Viana, "Estimating the active and reactive power flexibility area at the tso-dso interface," *IEEE Transactions on Power Systems*, vol. 33, no. 5, pp. 4741–4750, 2018.

[18] F. Capitanescu, "Computing cost curves of active distribution grids aggregated flexibility for tso-dso coordination," *IEEE Transactions on Power Systems*, vol. 39, no. 1, pp. 2381–2384, 2024.

[19] A. Churkin, M. Sanchez-Lopez, M. I. Alizadeh, F. Capitanescu, E. A. Martínez Ceseña, and P. Mancarella, "Impacts of distribution network reconfiguration on aggregated der flexibility," in *2023 IEEE Belgrade PowerTech*, 2023, pp. 1–7.

[20] D. A. Contreras and K. Rudion, "Impact of grid topology and tap position changes on the flexibility provision from distribution grids," in *2019 IEEE PES Innovative Smart Grid Technologies Europe (ISGT-Europe)*, 2019, pp. 1–5.

[21] M. Baran and F. Wu, "Network reconfiguration in distribution systems for loss reduction and load balancing," *IEEE Transactions on Power Delivery*, vol. 4, no. 2, pp. 1401–1407, 1989.

[22] R. D. Zimmerman, C. E. Murillo-Sánchez, and R. J. Thomas, "Matpower: Steady-state operations, planning, and analysis tools for power systems research and education," *IEEE Transactions on Power Systems*, vol. 26, no. 1, pp. 12–19, 2011.